3D MICROSTRUCTURAL EFFECTS ON PLANE STRAIN DUCTILE CRACK GROWTH

Alan Needleman*, Viggo Tvergaard**
*Division of Engineering, Brown University, Providence, RI 02912, USA
**Department of Mechanical Engineering, The Technical University of Denmark, 2800 Lyngby, Denmark

Summary Ductile crack growth under mode I, plane strain, small scale yielding conditions is analyzed. Overall plane strain loading is prescribed, but a full 3D analysis is carried out to resolve microstructural effects. An elastic-viscoplastic constitutive relation for a porous plastic solid is used to model the material. Two populations of second phase particles are represented, large inclusions with low strength, which result in large voids near the crack tip at an early stage, and small second phase particles, which require large strains before cavities nucleate. The larger inclusions are represented discretely and the effect of their 3D distribution on the crack path and on the overall crack growth rate is analyzed.

INTRODUCTION

In a wide variety of circumstances of practical interest, the stress and deformation fields near a crack tip in a structural metal, but outside the fracture process zone, are appropriately idealized as plane strain fields. However, the material microstructure in the process zone, which sets the plane strain crack growth resistance is inherently three dimensional. The main mechanism of ductile fracture in the process zone is void nucleation, growth and coalescence, and the spacing and distribution of void nucleating inclusions is the key microstructural feature for setting the crack growth resistance. Typically, for structural metals, the size of the void nucleating particles ranges from 0.1 μm to 100 μm, with volume fractions of a few percent. Quite commonly, the distribution of void nucleating particles can be idealized as involving two size scales; larger particles (e.g. MnS inclusions in steels) that nucleate voids at relatively small strains and smaller particles (e.g. carbides in steels) that nucleate voids at much larger strains. It is well appreciated that the distribution of inclusions plays a major role in setting the crack growth resistance in such materials, and while there have been a few 3D analyses of porosity induced ductile crack growth, e.g. Ruggieri *et al*. [1] and Hao and Brocks [2], full 3D analyses quantifying the role of inclusion distribution on crack growth behavior have not been carried out.

The analyses are carried out using a constitutive framework for progressively cavitating ductile solids stemming from the work of Gurson [3]. In this constitutive relation, the porosity is represented in terms of a single scalar parameter, the void volume fraction. The matrix material is modeled as an isotropic hardening viscoplastic solid. The large inclusions which nucleate voids at an early stage are modeled as a distribution of 'islands" of the amplitude of the void nucleation function. Thus, their size and spacing are directly specified in the analyses and introduce a characteristic length into the formulation. The smaller second-phase particles, which require large strains for nucleation, are uniformly distributed. This formulation has been used to carry out analyses of crack growth for 2D model microstructures, e.g. Tvergaard and Needleman [4], where the larger inclusions could only be represented as long cylinders, which is not geometrically realistic. It was shown in Needleman and Tvergaard [5] that in cases where the voids nucleated from the larger inclusions dominate the fracture process, the crack growth predictions exhibited practically no mesh sensitivity.

The same material model is used as in previous 2D studies, e.g. [4], but here 3D microstructures are analyzed. A slice of material with an initial crack is analyzed. Overall plane strain conditions are imposed and various distributions of larger spherical inclusions are specified. The calculations are for small scale yielding conditions with remote mode I loading, with a monotonically increasing stress intensity factor prescribed. The analyses account for finite deformations. For numerical efficiency, transient analyses are carried out, but the initial conditions and loading rate are chosen so that inertial effects are negligible. Although overall plane strain conditions are prescribed, the stress and deformation states that develop in the fracture process zone are fully three dimensional.

FORMULATION

A convected coordinate Lagrangian formulation is used with the dynamic principle of virtual work written as

$$\int_V \tau^{ij}\delta E_{ij}\,dV = \int_S T^i \delta u_i\,dS - \int_V \rho\frac{\partial^2 u^i}{\partial t^2}\delta u_i\,dV \tag{1}$$

where E_{ij} are the covaraiant Lagrangian strain components, τ^{ij} are the contravariant components of Kirchhoff stress on the deformed convected coordinate net, T^i are the contravariant components of nominal traction, ν_j and u_j are the covariant components of the reference surface normal and displacement vectors, respectively, ρ is the mass density, and V and S are the volume and surface of the body in the reference configuration.

With the origin of the coordinate system at the crack tip, the region analyzed is defined by $-W \le y^1 \le W$, $0 \le y^2 \le L$ and $0 \le y^3 \le H$ and the boundary conditions imposed are that $u_3 = 0$ on $y^3 = 0$ and $y^3 = H$ (giving overall plane strain); $u_2 = 0$ on $y^2 = 0$, $y^1 > 0$. The loading is prescribed through u_1 and u_2 on $y^1 = \pm W$ and $y^2 = L$ which are given by the plane strain mode I crack tip displacement fields. The mode I stress intensity factor, which is the amplitude of these displacements, is the prescribed quantity. The parts of the boundary where displacements are not prescribed, including of course the crack surface, are traction free. Also, the initial crack tip is taken to be a wedge-shaped notch.

The constitutive framework is the modified Gurson [3] flow potential given by

$$\Phi = \frac{\sigma_e^2}{\bar{\sigma}^2} + 2q_1 f^* \cosh\left(\frac{3q_2\sigma_h}{2\bar{\sigma}}\right) - 1 - (q_1 f^*)^2 = 0 \tag{2}$$

Here, σ_e is the effective stress, σ_h is the hydrostatic stress, $\bar{\sigma}$ is the matrix flow strength and the function f^* accounts for the effects of rapid void coalescence at failure

$$f^* = \begin{cases} f & f < f_c \\ f_c + (1/q_1 - f_c)(f - f_c)/(f_f - f_c) & f \geq f_c \end{cases} \tag{3}$$

where f is the void volume fraction. This constitutive relation and background on the basis for the choice of parameter values in it is discussed in Tvergaard [6].

The constitutive relation for the matrix material includes strain and strain rate hardening and thermal softening, with adiabatic conditions assumed. The crack growth mechanism analyzed involves two populations of void nucleating particles; large particles that nucleate voids at relatively small strains and smaller particles that nucleate voids at much larger strains. The small scale particles are taken to be uniformly distributed and nucleate by a plastic strain controlled mechanism. The large inclusions are modeled as constant amplitude spherical "islands" of stress-controlled void nucleation. The constitutive relation is such that the stress carrying capacity vanishes when f^* reaches a critical value. The initiation of crack growth as well as the subsequent rate and direction of crack growth are directly determined by the evolution of material failure.

Twenty node brick elements are used with eight point integration. The equations resulting from substituting the finite element discretization of the principle of virtual work (1) are integrated numerically by an explicit integration procedure. The mesh used has $71,424$ elements, $314,279$ nodal points and $942,837$ degrees of freedom.

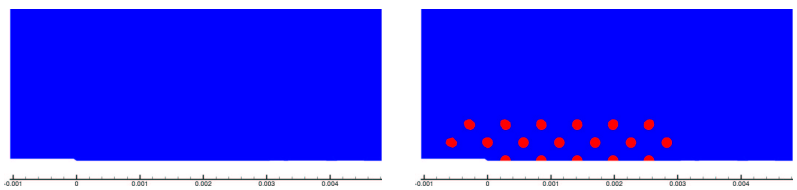

Figure 1. Contours of the amplitude of stress-controlled void nucleation in the near crack tip region showing the inclusion distribution for two slices of y^3 =constant.

RESULTS

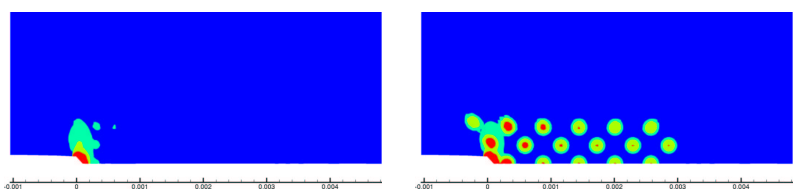

Figure 2. Contours of void volume fraction in the near crack tip region for the two slices of y^3 =constant in Fig. 1.

Calculations are carried out for various distributions of larger inclusions, with material parameter values representative of a structural steel. Figure 1 shows the distribution of the amplitude of stress-controlled void nucleation for one distribution. In one slice, corresponding to $y^3 = H/2$ no inclusions are present whereas a distribution of inclusions is seen in the slice at $y^3 = 0$, thus illustrating the three dimensional nature of the distribution. As a consequence of this inclusion distribution, crack growth does not occur in a uniform planar manner as seen from the contours of void volume fraction in Fig. 2 which shows a stage near the initiation of crack growth. The implications of the 3D inclusion distribution for the initiation of crack growth, for the evolution of the crack path and for the material's crack growth resistance are illustrated and discussed.

References

[1] Ruggieri T.L., Panontin T.L., Dodds R.H.: *Int. J. Fract.* **82**:67-95, 1996.
[2] Hao S., Brocks W.: *Comp. Mech.* **20**:34-40, 1997.
[3] Gurson A.L.: Plastic Flow and Fracture Behavior of Ductile Materials Incorporating Void Nucleation, Growth and Interaction. *PhD Thesis*, Brown University, 1975.
[4] Tvergaard V., Needleman A.: *J. Mech. Phys. Solids* **40**:447-471, 1992.
[5] Needleman A., Tvergaard, V.: *Engin. Fract. Mech.* **47**:75-91, 1994.
[6] Tvergaard, V.: *Adv. Appl. Mech.* **27**:83-151, 1990.